1 **Aryl Hydrocarbon Receptor Directly Regulates *Artemin* Gene Expression**

2

3 Tomohiro Edamitsu[a,b], Keiko Taguchi[a], Eri H. Kobayashi[a], Ryuhei Okuyama[b], and
4 Masayuki Yamamoto[a,*]
5 [a]Department of Medical Biochemistry, Tohoku University Graduate School of Medicine,
6 2-1 Seiryo-machi, Aoba, Sendai 980-8575, Japan, [b]Department of Dermatology,
7 Shinshu University Graduate School of Medicine, 3-1-1 Asahi, Matsumoto, Nagano
8 390-8621, Japan.

9

10 ***Corresponding author:**
11 Masayuki Yamamoto, M.D., Ph.D.
12 2-1 Seiryo-machi, Aoba, Sendai 980-8575, Japan
13 TEL: +81-22-717-8089
14 FAX: +81-22-717-8090
15 masiyamamoto@med.tohoku.ac.jp

16

17 **Running title: AhR-Artemin axis in alloknesis**
18 **Word count for the Materials and Methods:** 1,192 words
19 **Word count for the Introduction, Results, Discussion and Figure Legends:** 5,040
20 words
21 **KEYWORDS:** AhR, Artemin, Skin, Alloknesis, Atopic dermatitis

22

ABSTRACT

Transgenic mice expressing a constitutively active form of the aryl hydrocarbon receptor in keratinocytes (AhR-CA mice) develop severe dermatitis that substantially recapitulates the pathology of human atopic dermatitis. The neurotrophic factor Artemin (Artn) is highly expressed in the epidermis of AhR-CA mice and causes hypersensitivity to itch (alloknesis) by elongating nerves into the epidermis. However, whether the *Artn* gene is regulated directly by AhR or indirectly through complex regulation associated with AhR remains unclear. To this end, we previously conducted chromatin immunoprecipitation-sequencing analyses of the *Artn* locus and found a xenobiotic response element (XRE) motif located far upstream (52 kb) of the gene. Therefore, in this study, we addressed whether the XRE actually regulates the *Artn* gene expression by deleting the region containing the motif. We generated two lines of $Artn^{\Delta XRE}$ mice. In the mouse epidermis, inducible expression of the *Artn* gene by the AhR agonist 3-methylcholanthrene was substantially suppressed compared with that in wild-type mice. Importantly, in AhR-CA::$Artn^{\Delta XRE}$ mice, *Artn* expression was significantly suppressed, and alloknesis was improved. These results demonstrate that the *Artn* gene is indeed regulated by the distal XRE-containing enhancer, and alloknesis in AhR-CA mice is provoked by the AhR-mediated direct induction of the *Artn* gene.

42 **INTRODUCTION**

43 Aryl hydrocarbon receptor (AhR) is a ligand-dependent transcription factor that belongs
44 to the basic helix-loop-helix (bHLH) Per-Arnt-Sim (PAS) family (1). Polyaromatic
45 hydrocarbons (PAHs), which are one of the major air pollutants generated by the
46 incomplete combustion of organic materials, such as fossil fuels, are typical ligands for
47 AhR (2, 3). Following ligand binding, AhR undergoes a conformational change,
48 resulting in its translocation into the nucleus. Nuclear AhR binds to the aryl
49 hydrocarbon receptor nuclear translocator (Arnt), and the AhR-Arnt heterodimer
50 directly binds to the xenobiotic response element (XRE), which enhances target gene
51 transcription. The minimum core consensus sequence of XRE is 5'-CACGC-3' (4),
52 and the expression of *Cyp1a1*, a prominent AhR target gene, has been used as an
53 elaborate indicator of AhR activation (5, 6).

54 Atopic dermatitis (AD) is a chronic inflammatory skin condition that includes
55 severe pruritus and eczema. Exposure to air pollutants has been reported as one of the
56 risk factors associated with the development of AD (7–11). To analyze the effects of
57 chronic exposure to air pollutants on the skin, we generated transgenic mouse lines
58 expressing a constitutively active form of AhR (AhR-CA) under the control of the
59 promoter of the gene encoding *Keratin 14*, which is expressed exclusively in
60 keratinocytes (12). Importantly, the AhR-CA mouse exhibits a phenotype similar to
61 that of human AD patients with severe eczema and frequent scratching, implying that
62 the constitutive activation of the AhR regulatory pathway may provoke pathological
63 conditions similar to those frequently observed in AD patients. We previously found
64 the marked transactivation of the neurotrophic factor Artemin (Artn) in AhR-CA mouse
65 skin, which caused alloknesis by elongating nerves into the epidermis (13). Alloknesis,

66 a touch-evoked itch in which even mild mechanical stimulation triggers pruritus, is a
67 characteristic of the skin of AD patients (14). Innocuous mechanical stimuli to the
68 skin of AD patients, such as clothes that contact the skin, easily evoke scratching.
69 Scratching further damages the skin barrier, worsening symptoms and significantly
70 impairing the quality of life of patients (15).

71 Artn is a member of the glial cell-derived neurotrophic factor (GDNF)-related
72 family that promotes the survival, proliferation and neurite outgrowth of neurons by
73 binding to GDNF family receptor α3 (Gfrα3) (16). To date, little is known about the
74 molecular mechanisms that regulate *Artn* gene and protein expression. In the skin, the
75 overexpression of *Artn* in the epidermis induces the expression of transient receptor
76 potential cation channel subfamily V1 (TRPV1) and A1 (TRPA1) in cutaneous sensory
77 neurons, leading to hypersensitivity to cold and warm stimuli (17). We demonstrated
78 that Artn is an important regulatory factor for extending TRPV1-positive peripheral
79 nerves in the skin, since the subcutaneous administration of an Artn-neutralizing
80 antibody suppresses peripheral nerve elongation into the epidermis and blocks
81 alloknesis in AhR-CA mice (13).

82 Based on a few observations, we hypothesized that the *Artn* gene may be
83 controlled by the AhR regulatory pathway. First, we previously reported that
84 7,12-dimethylbenz[a]anthracene (DMBA), which is one of the PAHs that activate AhR,
85 upregulated the *Artn* gene expression *in vivo* (13). Second, human ARTN expression
86 is positively correlated with CYP1A1 expression in the epidermis of AD patients (13).
87 Third, in chromatin immunoprecipitation-sequencing (ChIP-seq) analyses, AhR-CA
88 binds to a region that may retain regulatory influence for the *Artn* gene, and this region
89 contains one copy of XRE (13). However, the XRE-containing region resides

90 approximately 52 kb from the transcription start site (TSS) of the *Artn* gene and is
91 located in an intron of another gene, ST3 β-galactoside α-2,3-sialyltransferase 3
92 (*St3gal3*). Therefore, this hypothesis needs to be tested rigorously by *in vivo*
93 transactivation studies.

94 To address whether AhR directly upregulates *Artn* gene expression by binding to
95 an XRE-containing region in AhR-CA mouse skin, which mimics prolonged exposure
96 to air pollutants and the development of AD, in this study, we tried a targeted knockout
97 of the XRE-containing region. We generated two lines of mice harboring deletions in
98 the XRE-containing region ($Artn^{\Delta XRE}$ mice) by means of CRISPR/Cas genome-editing
99 technology and examined whether AhR and the XRE-containing region directly regulate
100 the *Artn* gene. Our results clearly demonstrate that the XRE-containing region, located
101 more than 50 kb from the *Artn* gene, acts as an enhancer that drives *Artn* gene
102 expression in the skin, and we refer to this region as the *Artn* distal enhancer.
103

104 **RESULTS**

105 **AhR agonist induces *Artn* gene expression.** To address AhR-dependent *Artn*
106 gene expression, we first investigated whether a representative AhR agonist,
107 3-methylcholanthrene (3-MC), induces *Artn* gene expression *in vivo* in
108 epidermis-specific *AhR* knockout (Keratin5-Cre::AhR$^{flox/flox}$; K5Cre-AhR) mice and
109 control K5Cre mice. Notably, 3-MC binds to AhR and stimulates the transcription of
110 target genes via XRE (18). We applied 3-MC or acetone (vehicle) to the skin of
111 control K5Cre mice and K5Cre-AhR mice at the postnatal age of 4 days (P4). In the
112 epidermis of control mice, the expression of *Artn* and *Cyp1a1*, a typical AhR target gene,
113 was upregulated approximately 7- and 30-fold, respectively, at 24 h after the topical
114 application of 3-MC (Fig. 1A). In contrast, in the epidermis of 3-MC-treated
115 K5Cre-AhR mice, the expression of *Artn* and *Cyp1a1* was not induced because of the
116 lack of AhR.

117 We then examined Artn protein expression in the skin via immunohistochemistry.
118 The 3-MC treatment increased the expression of both Artn and Cyp1a1 proteins in the
119 epidermal layer of control mouse skin, but the vehicle treatment did not induce the
120 expression of either protein (Fig. 1B). Importantly, both Artn and Cyp1a1 proteins
121 were not detected in the K5Cre-AhR mouse skin, even after 3-MC treatment. The
122 vehicle treatment did not show any changes in either control or K5Cre-AhR mice.
123 These results thus suggest that the *Artn* gene expression in the mouse skin was
124 transcriptionally upregulated by 3-MC-induced AhR.

125

126 **Identification of an XRE-containing enhancer in the *Artn* gene and the**
127 **generation of Artn$^{\Delta XRE}$ transgenic mice.** To determine whether *Artn* gene expression

128 is under the direct regulation of AhR or under the indirect regulation of complexes
129 associated with AhR, we previously conducted comprehensive ChIP-seq analysis using
130 a hemagglutinin (HA) antibody, which detects HA tag-fused AhR-CA protein (13).
131 The analysis exploiting the epidermis of AhR-CA mice led to the identification of an
132 AhR-CA binding site located far upstream of the *Artn* gene. Through closer inspection
133 of the binding region, we indeed found an XRE sequence, suggesting that AhR might
134 regulate *Artn* gene expression through binding to the XRE site in the far upstream
135 enhancer. However, the XRE is located approximately 52 kb from the TSS of the *Artn*
136 gene. Moreover, the enhancer region containing the XRE site is located in an intron of
137 the *St3gal3* gene. Therefore, we realized that the potential direct regulation of the *Artn*
138 gene by AhR needs to be verified through an experimental approach.

139 To examine the direct control of *Artn* gene expression by AhR through the XRE *in*
140 *vivo*, we generated two lines of mice harboring an XRE deletion by using the
141 CRISPR/Cas genome-editing approach (Fig. 2A). We designed a pair of guide RNAs
142 (gRNAs) to delete the region, including the XRE (Fig. 2B), and obtained 2 mutant lines.
143 Genomic DNA sequencing identified deletions of 128 bp (Line #1) and 126 bp (Line
144 #2) genomic regions, including the XRE (Fig. 2B). The PCR products for the
145 wild-type (WT) and $Artn^{\Delta XRE/\Delta XRE}$ ($Artn^{\Delta XRE}$) mice were 483 bp (WT), 355 bp (Line #1)
146 and 357 bp (Line #2) in size by electrophoresis (Fig. 2C). These two lines of $Artn^{\Delta XRE}$
147 mice showed normal growth rates and appeared to be healthy, indicating that we
148 succeeded in generating 2 lines of $Artn^{\Delta XRE}$ mice.

149

150 **Induction of *Artn* gene expression by 3-MC via the AhR-XRE axis.** To clarify
151 XRE-dependent *Artn* gene expression, we investigated whether 3-MC could induce *Artn*

152 expression in Artn$^{\Delta XRE}$ mice (Line #1). We applied 3-MC or acetone (vehicle) to the
153 skin of control WT and Artn$^{\Delta XRE}$ mice at P4, P14 and P24 (Fig. 3; upper panel). Gene
154 expression levels were compared with vehicle-treated WT mice at P4. The expression
155 of the *Artn* gene in the epidermis of WT mice was upregulated approximately 13-, 26-
156 and 37-fold at P4, P14 and P24, respectively, 24 h after the topical application of 3-MC.
157 In contrast, the induction of gene expression by 3-MC in the epidermis of Artn$^{\Delta XRE}$ mice
158 at P4, P14 and P24 was reduced approximately 5-, 7- and 12-fold, respectively, which
159 were markedly lower than that in the epidermis of WT. The gene expression levels in
160 vehicle-treated WT mice at P4 were comparable to those at P14 and P24.

161 The expression of *Cyp1a1* was upregulated 49-, 24- and 37-fold in WT mice at P4,
162 P14 and P24, respectively, after 3-MC application (Fig. 3; middle panel). The
163 induction of *Cyp1a1* expression by 3-MC in the epidermis of Artn$^{\Delta XRE}$ mice at P4, P14
164 and P24 was upregulated approximately 56-, 27- and 44-fold, respectively. The
165 expression levels of *Cyp1a1* did not change substantially between the WT and Artn$^{\Delta XRE}$
166 mice at three time points. We also examined the expression levels of *St3gal3* and
167 found that there was no alteration in the deletion of XRE or the application of 3-MC in
168 both WT and Artn$^{\Delta XRE}$ mice at P4, P14 and P24 (Fig. 3; lower panel). This result
169 indicates that the enhancer resides in the intron of the *St3gal3* gene and that the XRE
170 sequence does not regulate *St3gal3* gene expression but strongly induces the expression
171 of the *Artn* gene *in vivo*. These results thus demonstrate that the contribution of the
172 *Artn* distal enhancer to *Artn* gene expression is quite reproducible in the epidermis of P4,
173 P14 and P24 mice, while the expression levels of the *Artn* gene progressively increase
174 with age.

175 An important observation here is that the contribution of the *Artn* distal enhancer

176 with an XRE is predominant; a loss-of-the-enhancer-function mutation elicits the loss of
177 almost two-thirds of *Artn* gene expression, and this level of contribution from the
178 enhancer is maintained at a constant level throughout the developmental stage of
179 juvenile mice. These results suggest that there may also be independent but minor
180 regulatory pathways for the expression of the *Artn* gene. The progressive increase in
181 *Artn* gene expression with age further suggests the existence of additional regulatory
182 pathways.
183
184 **Loss of the AhR binding to the *Artn* distal enhancer in Artn$^{\Delta XRE}$ mouse skin.**
185 We previously revealed that AhR-CA bound to the distal XRE located approximately 52
186 kb from the TSS of the *Artn* gene by ChIP-seq and ChIP-qPCR analyses (13).
187 However, it remains unclear whether endogenous AhR also binds to the region. To
188 verify the binding of AhR, we performed a ChIP-qPCR analysis using 3-MC treated
189 epidermis of WT and Artn$^{\Delta XRE}$ mice (Fig. 4). In the epidermis of WT mice, the
190 binding signal of AhR to the distal enhancer region was significantly higher than that of
191 IgG, a negative control antibody. In contrast, the AhR signal did not increase in
192 Artn$^{\Delta XRE}$ mice. These results demonstrate that endogenous AhR also activated *Artn*
193 gene transcription via binding to the distal enhancer. Together with the results in
194 Figure 3, the data clearly show that AhR bound to the *Artn* distal enhancer regulates
195 *Artn* gene expression.
196
197 **Decrease in Artn protein expression by 3-MC in Artn$^{\Delta XRE}$ mouse skin.**
198 Following examination of *Artn* mRNA expression, we also analyzed Artn protein
199 expression in the skin via immunohistochemistry. Treatment with 3-MC increased

200 both Artn and Cyp1a1 protein levels in the epidermal layer of the skin in control mice
201 at P4 (Fig. 5). While the Artn level was decreased and marginally detected in
202 3-MC-treated Artn$^{\Delta XRE}$ mouse skin, Cyp1a1 was clearly detected in 3-MC-treated
203 Artn$^{\Delta XRE}$ mouse skin at levels almost comparable to those in WT mouse skin. The
204 application of the vehicle did not show any changes in either control or Artn$^{\Delta XRE}$ mice.
205 These results clearly demonstrate that AhR directly upregulates *Artn* gene expression
206 via XRE in the *Artn* distal enhancer and increases the expression of the gene product in
207 the epidermis.
208
209 **Induction of *Artn* via the AhR-XRE axis in AhR-CA mice.** We previously
210 generated two lines of AhR-CA mice expressing the constitutively active form of AhR
211 in keratinocytes (12). In the epidermis of these AhR-CA mice, AhR activity was
212 constitutively enhanced in the absence of ligands, and the *Artn* gene was substantially
213 activated in the epidermis of AhR-CA mice (13). To address how the loss of the
214 distal enhancer affects the expression of the *Artn* gene in AhR-CA mice, we crossed
215 Artn$^{\Delta XRE}$ mice with AhR-CA mice to generate AhR-CA::Artn$^{\Delta XRE}$ mice. This
216 cross-breeding strategy is shown in Figure 6A.
217 To follow up with broad-range phenotypes, in this analysis, we utilized P4 and
218 11-week-old (11W) mice. At both P4 and 11W, expression of the *Artn* gene was
219 increased in the epidermis of AhR-CA mice (Fig. 6B; left panels) but reduced in the
220 epidermis of AhR-CA::Artn$^{\Delta XRE}$ mice. An intriguing observation is that the
221 expression of the *Artn* gene was induced more than 21-fold by the constitutive
222 activation of AhR in the epidermis of P4 mice, and this induction could not be
223 completely canceled by the deletion of the distal enhancer. There was a significant

224 difference in the expression of *Artn* mRNA between WT and AhR-CA::Artn$^{\Delta XRE}$
225 mice; almost 7-fold induction remained. In contrast, while there was an induction of
226 *Artn* gene expression by the constitutively active expression of AhR at 11W, the
227 magnitude of the induction was approximately 8-fold, which is much lower than that
228 in the mouse epidermis at P4, and the level of *Artn* mRNA returned to the WT level by
229 the deletion of the distal enhancer in 11W mouse epidermis. These results imply that
230 there are additional regulatory influences on the expression of the *Artn* gene that may
231 be prevalent in the epidermis of P4 stage mice.

232 We confirmed that *Cyp1a1* gene upregulation was comparable between P4 and
233 11W AhR-CA mice (Fig. 6B; middle panels). The upregulation of *Cyp1a1* gene
234 expression was similar in AhR-CA and AhR-CA::Artn$^{\Delta XRE}$ mice, indicating that
235 *Cyp1a1* gene expression was not affected by the deletion of the *Artn* distal enhancer.
236 The expression of *St3gal3* was also not altered by deleting the XRE (Fig. 6B; right
237 panels). These results thus demonstrate that *Artn* gene induction in the AhR-CA
238 mouse epidermis was significantly reduced by the targeted deletion of the enhancer,
239 supporting the contention that *Artn* gene expression in the AhR-CA mouse epidermis
240 is indeed under the regulation of the *Artn* distal enhancer.

241

242 **Loss of the *Artn* distal enhancer improves alloknesis in AhR-CA mice.**
243 AhR-CA mice (line 239) spontaneously develop AD-like skin lesions and frequent
244 scratching with alloknesis (12, 13). Available lines of evidence suggest that the
245 high-level of Artn expression is responsible, at least in part, for the pathogenesis of
246 AD-like skin lesions (13). To address how the loss of the *Artn* distal enhancer
247 improves the AD-like phenotype in AhR-CA mice, we assessed the clinical severity of

248 dermatitis. Skin lesions first appeared at 2 to 4 weeks after birth in AhR-CA and
249 AhR-CA::Artn$^{\Delta XRE}$ mice and were gradually aggravated with age. There was no
250 significant difference in the severity of dermatitis between these two groups of mice by
251 11W (Fig. 7A). In contrast, no skin lesions developed in WT and Artn$^{\Delta XRE}$ mice.
252 To address how the loss of *Artn* gene expression by the deletion of the *Artn* distal
253 enhancer improved alloknesis in AhR-CA mice, we attempted the von Frey test, which
254 mechanically irritated the mouse skin and induced itch. To avoid the obvious
255 influence of dermatitis, we conducted this analysis using 4-week-old (4W) mice in
256 which dermatitis was not very apparent. Innocuous tactile stimulation with a von Frey
257 filament induced scratching in neither WT nor Artn$^{\Delta XRE}$ mice at 4W (Fig. 7B). In
258 contrast, light stimulation of the skin elicited severe scratching in the AhR-CA mice.
259 Notably, this stimulation-induced scratching was significantly diminished in
260 AhR-CA::Artn$^{\Delta XRE}$ mice, indicating that the *Artn* distal enhancer contributes to the
261 establishment of alloknesis in AhR-CA mice.
262
263 **Artn-neutralizing antibody reduces continuous scratching behavior in**
264 **AhR-CA mice.** While the *Artn* gene expression in AhR-CA::Artn$^{\Delta XRE}$ mice was lower
265 than that in AhR-CA mice, the expression level was still approximately 7-fold higher
266 than that in WT mice at P4 (see Fig. 6B). This observation suggested that there may
267 be other contributions of Artn in the AhR-CA::Artn$^{\Delta XRE}$ mouse epidermis. To clarify
268 how significantly Artn upregulation contributes to the AD-like phenotype of AhR-CA
269 mice, we administered an Artn-neutralizing antibody (Artn-ab) or IgG2a antibody
270 (control) to AhR-CA mice. As described in the Introduction section, our previous
271 study revealed that Artn-ab ameliorates alloknesis in AhR-CA mice at 4W (13). In this

272 study, to follow up with broad-range phenotypes, we evaluated the clinical severity of
273 dermatitis and spontaneous scratching behavior for up to 11W. The Artn-ab blocks
274 Artn-Gfrα3 interactions (19). Skin lesions appeared at 2 to 4 weeks after birth and
275 gradually aggravated with age in both control- and Artn-ab-injected AhR-CA mice.
276 There was no significant difference in the severity of dermatitis between these two
277 groups of mice by 11W (Fig. 8A). No skin lesions developed in control- or Artn-ab-
278 injected WT mice.

279 We monitored the scratching behaviors of the four groups of mice. Figure 8B
280 shows the results of two representative analyses for each group of mice. We did not
281 find any significant scratching in WT mice with or without control- or Artn-ab- injection.
282 In contrast, continuous scratching behavior was observed in AhR-CA mice treated with
283 the control antibody, which indicated the presence of alloknesis. Notably, the injection
284 of Artn-ab markedly reduced the consecutive scratching in the AhR-CA mice.

285 Figure 8C demonstrates that the administration of Artn-ab significantly improved
286 the scratching behavior of AhR-CA mice, supporting the notion that the *Artn* gene
287 contributes to the characteristic continuous scratching behavior in AhR-CA mice.
288 These results thus indicate that the development of AD-like dermatitis in AhR-CA mice
289 is attributable to multiple AhR downstream pathways and that the Artn-scratching
290 pathway is one of the important cascades leading to AD-like dermatitis.

291

292 **DISCUSSION**

293 To elucidate how *Artn* gene expression is upregulated in the AhR-CA mouse
294 epidermis, we previously examined the mouse *Artn* gene and identified an *Artn* distal
295 enhancer that harbors one copy of XRE (13). This enhancer resides 52 kb from the
296 TSS of the *Artn* gene. To evaluate the contribution of the enhancer and the XRE, in
297 this study, we deleted the XRE and some surrounding sequences and established the
298 $Artn^{\Delta XRE}$ mouse lines, which enabled us to study the contribution of the distal enhancer
299 and XRE. As summarized in Figure 9, our results revealed that the pharmacological
300 and genetic activation of AhR in the epidermis upregulates *Artn* gene expression
301 through the *Artn* distal enhancer containing XRE. The inducible expression of *Artn*
302 via this enhancer provokes alloknesis in mice, which contributes, at least in part, to the
303 pathogenesis of AD-like dermatitis.

304 Mechanisms of transcriptional enhancement through the AhR-XRE axis have been
305 well characterized using *CYP1* genes that are representative AhR targets (4, 20–22).
306 Both *CYP1A1* and *CYP1B1* have several XREs within approximately 1 kb sequences
307 upstream of each gene, indicating that AhR utilizes juxtaposed XREs and enhancers.
308 Similarly, a ChIP-seq analysis using 2,3,7,8-tetrachlorodibenzo-p-dioxin
309 (TCDD)-treated MCF-7 human breast cancer cells revealed that the peak densities of
310 AHR and ARNT are highest within a 1 kb from the TSS, supporting the notion that
311 many AhR target genes are regulated by AhR binding to the proximal promoters (23).
312 One salient exception is the *AHR repressor* (*AHRR)* gene, another well-known AhR
313 target gene. *AHRR* has a functional XRE located approximately 17 kb downstream of
314 the TSS, which is distal compared to the other important AhR target genes (24). Our
315 present results provide another salient example that the AhR-XRE axis has the potential

316 to regulate target gene expression by binding to the distal XRE located more than 50 kb
317 away. Importantly, in an inspection of the abovementioned ChIP-seq data (23), we
318 have noticed several genes that harbor distant AHR-ARNT co-binding regions within
319 100 kb from the TSS, but the functional significance of the peak regions awaits further
320 characterization.

321 To the best of our knowledge, this result is the first demonstration that the
322 transcription of the *Artn* gene is directly regulated by AhR through binding to XRE. In
323 this regard, we found that deletion of the *Artn* distal enhancer abrogated approximately
324 two-thirds of the *Artn* gene expression induced by 3-MC in $Artn^{\Delta XRE}$ mice at P4, P14
325 and P24, but almost one-third of the *Artn* gene expression remained in these mice.
326 This observation was reproducible in the AhR-CA::$Artn^{\Delta XRE}$ mice at P4, which harbor
327 the constitutively active expression of AhR combined with the *Artn* distal enhancer
328 deletion. In contrast, in 11W AhR-CA::$Artn^{\Delta XRE}$ mouse epidermis, the level of *Artn*
329 mRNA was comparable to that of WT mice, and the remaining activity disappeared.
330 While the precise regulation that maintains *Artn* gene expression in the absence of the
331 *Artn* distal enhancer in juvenile mice remains to be clarified, we surmise that the
332 following observations may be pertinent.

333 One plausible explanation for these observations is that there may be an additional
334 XRE. However, as we did not find any obvious peaks in our ChIP-seq analyses
335 within 50 kb upstream and downstream of TSS, we feel that this possibility is unlikely.
336 Alternatively, there may be additional transcription activation pathways that lead to
337 *Artn* gene expression. It should be noted that the estrogen receptor (ER) has been
338 reported to regulate the expression of the *Artn* gene (25). Estrogen stimulation
339 induces the expression of *ARTN* in the ER-positive mammary carcinoma cell lines

340 MCF-7 and T47D (25). This induction has been shown to be ER-dependent in an
341 experiment exploiting the ER-negative mammary carcinoma cell line BT549 (25).
342 ERα and ERβ are ligand-activated transcription factors that belong to a nuclear
343 receptor superfamily. Intriguingly, there are interactions between the AhR and ER
344 signaling pathways (26). In fact, AhR ligands induce the formation of an AhR-ER
345 complex that binds to the estrogen response element (ERE) and stimulates the
346 transcription of ER target genes (27, 28). ERs are expressed in keratinocytes (29, 30).
347 Therefore, we surmise that ERs and related factors may be some of the candidates
348 responsible for the remaining *Artn* gene expression.

349 Available lines of evidence suggest that the high-level expression of Artn is
350 responsible, at least in part, for the pathogenesis of AD-like skin lesions (13). In this
351 study, we found that the deletion of the *Artn* distal enhancer did not result in complete
352 remission from AD symptoms. We surmise that the constitutive activation of AhR
353 may also evoke abnormalities in addition to nerve elongation into the epidermis that
354 depend on Artn overexpression. Nonetheless, we found that the suppression of *Artn*
355 gene expression induced by the deletion of the *Artn* distal enhancer improved
356 touch-evoked or spontaneous scratching behaviors in the AhR-CA::Artn$^{\Delta XRE}$ mice.
357 This finding shows very good agreement with our current and previous studies (13)
358 using an Artn-neutralizing antibody. Subcutaneous injection of the anti-Artn antibody
359 markedly reduced the consecutive scratching in the AhR-CA mice. Our results thus
360 demonstrate that alloknesis is suppressed at the local site in AhR-CA mice by the
361 Artn-suppression-mediated blocking of peripheral nerve elongation into the epidermis.

362 Itch is an important trigger of AD, and innocuous mechanical stimuli to the skin of
363 AD patients can easily evoke itching. Scratching further damages the skin barrier,

364 leading to inflammation in the skin. Currently, the common treatment for
365 AD-associated itch is the topical use of corticosteroids (31). The topical application of
366 corticosteroids inhibits inflammatory cytokines or chemokines, thereby decreasing local
367 inflammation and indirectly suppressing pruritus (32). However, novel therapeutic
368 drugs are required for AD patients who are steroid-ineffective or who have adverse
369 effects from steroids after long-term use. To this end, we hypothesized that controlling
370 the itch in AD patients by eliminating alloknesis is one of the important approaches in
371 the treatment of AD.

372 We envisage that the development of drugs that inhibit the activation of the
373 AhR-Artn axis is likely to proceed from the following two aspects. First, the blockade
374 of the Artn-induced neuronal extension appears to contribute to the elimination of the
375 molecular basis underlying the disease. Second, this approach may have good efficacy
376 in the treatment of patients with aggravated AD symptoms, especially those aggravated
377 by environmental pollutants.
378

379 **MATERIALS AND METHODS**

380 **Mice.** Transgenic mouse lines expressing the constitutively active form of AhR
381 (AhR-CA) conjugated with a hemagglutinin (HA) tag under the control of the *Keratin*
382 *14* gene promoter were generated as described (12). The AhR-CA mouse line 239 was
383 used in this study. A mouse line with loxP-flanked AhR alleles ($AhR^{flox/flox}$) on the
384 C57BL6/J background was supplied from Jackson Laboratory (33). A mouse line
385 expressing Cre recombinase from the epidermis-specific *Keratin 5* gene promoter
386 (Keratin 5-Cre; K5Cre) on the C57BL6/J background was kindly provided by Professor
387 Junji Takeda (Osaka University) (34). We crossed $AhR^{flox/flox}$ mice with K5Cre mice
388 to generate K5Cre::$AhR^{flox/flox}$ (K5Cre-AhR) mice on the C57BL6/J background.
389 AhR-CA mice were maintained on a mixed or ICR background. All mice were treated
390 according to the regulations of the Standards for the Human Care and Use of Laboratory
391 Animals of Tohoku University and the Guidelines for the Proper Conduct of Animal
392 Experiments of the Ministry of Education, Culture, Sports, Science, and Technology of
393 Japan. All animal experiments were conducted with the approval of the Tohoku
394 University Animal Care Committee.

395

396 **Generation of $Artn^{\Delta XRE}$ mice.** Based on the ChIP-seq data of AhR in AhR-CA
397 mouse keratinocytes, $Artn^{\Delta XRE}$ mice were designed and generated to delete the XRE
398 located 52 kb upstream of the *Artn* gene by CRISPR/Cas genome-editing technology.
399 *Cas9* mRNA, a pair of guide RNAs (gRNAs), and targeting oligonucleotides were
400 injected into fertilized eggs derived from BDF1 mice. The founder mice were crossed
401 with WT mice, and the mutations were transmitted to the germ line. The homozygotes
402 ($Artn^{\Delta XRE/\Delta XRE}$; $Artn^{\Delta XRE}$) were obtained by crossing the heterozygous mutants. The

403 Artn$^{\Delta XRE}$ mutant mice were identified by PCR (30 cycles at 94°C for 30 s, 60°C for 30 s,
404 and 72°C for 30 s) using the forward primer 5'-TCCCTCCTCTCCATTCCTCT-3' and
405 the reverse primer 5'-TACCCAGCCAGAGAAGCAGT-3'. The ChIP-seq analysis
406 data, GSE72449, were used in the Gene Expression Omnibus (GEO). We crossed
407 AhR-CA mice with Artn$^{\Delta XRE}$ mice to generate AhR-CA::Artn$^{\Delta XRE}$ mice on a mixed
408 background.
409
410 **DNA sequencing.** A genomic DNA region around the XRE located in the *Artn*
411 distal enhancer was amplified by PCR (30 cycles at 94°C for 30 s, 60°C for 30 s, and
412 72°C for 30 s) using the forward primer 5'-CAGGCTGCCTGTCAGATTCT-3' and the
413 reverse primer 5'-TACCCAGCCAGAGAAGCAGT-3'. The amplified samples were
414 then sequenced by ABI3100 (Applied Biosystems) using standard protocols.
415
416 **Exposure to 3-MC.** 3-MC (Sigma-Aldrich), a carcinogen in experimental animals
417 and human cells, was dissolved in acetone at a concentration of 0.04 mg/g body weight.
418 At 24 h after shaving, the male mice were anesthetized, and 3-MC or vehicle was
419 topically applied rostrally to their shaved backs. Samples of the epidermis at the
420 application sites were harvested 24 h after the application.
421
422 **cDNA synthesis and quantitative reverse transcription-PCR (RT-qPCR).** To
423 obtain murine epidermal samples, whole skin samples were incubated for 20 h at 4°C
424 with 0.5% (wt/vol) trypsin. The samples were then separated into epidermal and
425 dermal layers by peeling the layers apart. Total RNA was extracted from the epidermis
426 using Sepasol-RNA I Super G (Nacalai Tesque). cDNA was synthesized from total

427 RNA using ReverTra Ace qPCR RT master mix with gRNA Remover (TOYOBO).
428 RT-qPCR was performed by using a KAPA SYBR FAST qPCR Kit (Nippon Gene) with
429 the StepOne™ RT-PCR system (Applied Biosystems) or the QuantStudio 3 Real-Time
430 PCR system (Life Technologies). The data were normalized to *rRNA* expression.
431 Relative expression levels were determined using the $^{\Delta\Delta}$CT method. The primer
432 sequences used for RT-qPCR were as follows: *Artn*, forward
433 5'-AGACGGCCTCATAGCGAGT-3' and reverse
434 5'-CGAGCTGATACGTTTCCGCTT-3'; *Cyp1a1*, forward
435 5'-GGGTTTGACACAGTCACAACT-3' and reverse
436 5'-GGGACGAAGGATGAATGCCG-3'; *rRNA*, forward
437 5'-CGGCTACCACATCCAAGGAA-3' and reverse 5'-GCTGGAATTACCGCGGCT-3';
438 *St3gal3*, forward 5'-TGGGAAGACTCCAATTCATTGCT-3' and reverse
439 5'-AGTTTGCGTACTTGGTGGCT-3'.
440

441 **Chromatin immunoprecipitation (ChIP)-qPCR analyses.** WT and Artn$^{\Delta XRE}$
442 mice were treated with 3-MC for 24 h. Whole skins were incubated for 20 h at 4°C
443 with 0.5% (wt/vol) trypsin and then separated epidermal layers. The epidermis was
444 fixed with 1% (wt/vol) formaldehyde and quenched with glycine. Lysates were
445 sonicated with an ultrasonic homogenizer Sonifier 250 (Branson) to obtain chromatin
446 fragments 200–1000 bp in length. The protein, DNA and antibody complexes were
447 retrieved with Protein A- and Protein G-sepharose (GE healthcare). Chromatin lysate
448 was pre-cleared and incubated overnight with anti-AhR antibody (sc-5579, Santa Cruz
449 Biotechnology) and normal rabbit IgG (sc-2027, Santa Cruz Biotechnology). DNA
450 was purified using a phenol-chloroform extraction. To analyze protein-bound DNA,

451 primers for qPCR were used as follows: *Artn,* forward
452 5'-TCCCTCCTCTCCATTCCTCT -3' and reverse
453 5'-TACCCAGCCAGAGAAGCAGT-3'. qPCR was performed by using the KAPA
454 SYBR FAST qPCR Kit (Nippon Gene) with a QuantStudio 3 Real-Time PCR system
455 (Life Technologies). The percentage of the input that was bound was calculated.
456
457 **Histology.** Skin samples fixed in Mildform 10N (Wako Pure Chemical) were
458 embedded in paraffin and sectioned. For histological analysis, the samples were
459 stained with hematoxylin and eosin (HE). For immunohistochemistry, the sections
460 were reacted with anti-Cyp1a1 antibody (sc-9828, Santa Cruz Biotechnology) or
461 anti-Artn antibody (MAB10851; R&D Systems) overnight. Anti-Cyp1a1 antibody or
462 anti-Artn antibody binding was detected with a horseradish peroxidase-conjugated
463 anti-goat IgG antibody. The positive reactivity was visualized through
464 diaminobenzidine staining.
465
466 **Evaluation of dermatitis.** The clinical severity of dermatitis was assessed as
467 reported previously, with minor modifications (35). This scoring is based on the
468 severity of four possible symptoms (scaling, erosion, hemorrhage, and erythema) and
469 the area in which the skin lesions occurred. The degree of each symptom was scored
470 as 0 (no symptoms), 1 (mild), 2 (moderate) or 3 (severe). The area of the skin lesions
471 was scored as 1 for each location (face, rostral back and caudal back). The sum of the
472 individual scores (minimum: 0; maximum: 15) was taken as the dermatitis score.
473
474 **Measurement of scratching behavior.** Male mice were acclimated in an acrylic

475 cage for 10 min, and the frequency of scratching was measured for 10 min. According
476 to a previous paper (13, 36), scratching behavior was defined as movement of the hind
477 paw up to the back or face of the mouse. The behavior was considered finished when
478 the mouse placed its hind paw back on the floor. Continuous scratching behavior was
479 defined as scratching occurring at intervals of less than 5 s.
480
481 **Measurement of alloknesis.** Alloknesis scores were determined using a
482 previously reported method (13). The rostral part of the back of each male mouse was
483 shaved on the day before analysis. After an acclimation period of approximately 10
484 min in an acrylic cage, the mice received three separate innocuous mechanical
485 stimulations with a von Frey filament (0.16-g bending force) on the shaved regions of
486 their backs. This stimulation rarely elicited scratching behavior in WT mice. The
487 presence or absence of scratching behavior was recorded immediately after each
488 stimulus. These 3 innocuous stimuli were repeated three times at 5-min intervals (9
489 stimulations in total), and the alloknesis score was the total number of positive
490 responses.
491
492 **Artn-neutralization.** Male mice received a subcutaneous injection at 50 mg/kg
493 body weight of Artn-neutralizing antibody (MAB10851; R&D Systems) or IgG2a
494 antibody as a control (MAB006; R&D Systems) in the rostral part of the back once per
495 week from the first week to 11 weeks of age.
496

497 **Statistical analysis.** The average values were calculated, and the error bars
498 indicate the standard deviations (SD). The differences were analyzed using Student's
499 *t*-test. $P < 0.05$ was considered statistically significant.
500

ACKNOWLEDGMENTS

The authors would like to thank Dr. Masanobu Morita, Ms. Eriko Naganuma, Ms. Hiromi Suda and Ms. Nanae Osanai (Tohoku University) for technical support. This work was supported by funding from MEXT/JSPS KAKENHI [26111002 and 19H05649, M.Y.] and AMED-CREST, AMED [M.Y.] and the JSPS Research Fellowship for Young Scientists [19J10035, T.E.].

508 **FIGURE LEGENDS**

509 **FIG 1** An AhR agonist 3-MC induces *Artn* gene expression via AhR activation. (A)
510 Expression of *Artn* and *Cyp1a1* in the epidermis of K5Cre and K5Cre-AhR
511 (K5-Cre::AhR$^{flox/flox}$; epidermis-specific conditional AhR knockout) mice 24 h after
512 topical application of the vehicle (K5Cre or K5Cre-AhR, n=3 each) or 3-MC (K5Cre or
513 K5Cre-AhR, n=5 each) at the postnatal age of 4 days (P4). Note that the AhR
514 knockout substantially abolished *Artn* and *Cyp1a1* gene expression. The results are
515 presented relative to those of vehicle-treated K5Cre mice. Data represent the mean ±
516 SD. **P*<0.05 and ***P*<0.01 without a bar indicate the comparison to vehicle-treated
517 K5Cre mice. (B) Representative images of HE staining and Artn and Cyp1a1
518 immunostaining in control and K5Cre-AhR mice 24 h after the topical application of
519 vehicle or 3-MC. Scale bar, 50 μm.

520

521 **FIG 2** Generation of Artn$^{\Delta XRE}$ transgenic mice using the CRISPR/Cas system. (A)
522 Schematic illustration of the AhR-CA binding region in the *Artn* distal enhancer located
523 in an intron of the *St3gal3* gene, which is 52 kb upstream of the TSS of the *Artn* gene
524 including the XRE. These findings are based on ChIP-seq data using AhR-CA mouse
525 keratinocytes (13). (B) The DNA sequence around XRE core sequence, 5'-CACGC-3'
526 (red letters) in the AhR-CA binding region in chromosome 4, 117,982,819–117,982,973.
527 Positions of targeting gRNAs to generate the XRE-deleted mice (Artn$^{\Delta XRE}$ mice) via the
528 CRISPR/Cas system are indicated in blue letters. Protospacer adjacent motif (PAM)
529 sequences, CCT for gRNA are marked in green letters. Sequences of cleaved
530 fragments from Artn$^{\Delta XRE}$ mouse lines #1 and #2. PCR products from mouse DNA
531 samples were sequenced. In Artn$^{\Delta XRE}$ mouse lines #1 and #2, 128 bp and 126 bp were

532 deleted, respectively. The black lines indicate the deleted sequence. (C) Genotyping
533 analysis for WT and 2 lines of homogeneous Artn$^{\Delta XRE}$ mice. The genomic DNA from
534 WT and Artn$^{\Delta XRE}$ mice was amplified by PCR.
535
536 **FIG 3** AhR agonist 3-MC induces the *Artn* gene via the AhR-XRE axis. Expression
537 of *Artn, Cyp1a1* and *St3gal3* in the epidermis of WT and Artn$^{\Delta XRE}$ mice 24 h after the
538 topical application of 3-MC at P4, P14 and P24. Note that deletion of the XRE
539 substantially reduced *Artn* gene expression. Gene expression levels were compared
540 with vehicle-treated WT mice at P4. Data represent the mean ± SD (n=3-5).
541 **P*<0.05 and ***P*<0.01 without a bar indicate the comparison to vehicle-treated WT
542 mice at P4. n.s., not significant.
543
544 **FIG 4** Endogenous AhR binds to the *Artn* distal enhancer. ChIP-qPCR analysis of
545 the AhR binding at the 52 kb upstream of the *Artn* gene in 3-MC treated epidermis of
546 WT or Artn$^{\Delta XRE}$ mice. Note that the signal of AhR binding shows no increase in
547 Artn$^{\Delta XRE}$ mice. The percentage of the input was calculated. Data represent the mean
548 ± SD (n=4). ***P* < 0.01.
549
550 **FIG 5** 3-MC induces Artn protein expression in the epidermis via the AhR-XRE axis.
551 Representative images of HE staining and Artn and Cyp1a1 immunostaining of the
552 epidermis of WT and Artn$^{\Delta XRE}$ mice (P4) 24 h after the topical application of vehicle or
553 3-MC. Note that 3-MC induced Artn expression in the WT epidermis but not in the
554 Artn$^{\Delta XRE}$ mouse epidermis, while Cyp1a1 was induced in the epidermis of both
555 genotypes of mice. Scale bar, 50 μm.

556

557

558 **FIG 6** *Artn* gene expression is induced via the AhR-XRE axis in the epidermis of
559 AhR-CA mice. (A) Breeding scheme to generate AhR-CA::Artn$^{\Delta XRE}$ mice. Male
560 AhR-CA mice were crossed with female Artn$^{\Delta XRE}$ mice to obtain F1 mice. In F1,
561 double heterozygous male mice (AhR-CA::Artn$^{\Delta XRE/WT}$) were bred with female
562 Artn$^{\Delta XRE/WT}$ mice to generate the four genotypes on mixed background. (B)
563 Expression of *Artn, Cyp1a1* and *St3gal3* in the epidermis of WT (P4 or 11W; n=3 each),
564 Artn$^{\Delta XRE}$ (P4; n=5, 11W; n=7), AhR-CA (P4; n=4, 11W; n=6) and AhR-CA::Artn$^{\Delta XRE}$
565 mice (P4 or 11W; n=3 each). Note that deletion of the XRE substantially reduces *Artn*
566 gene expression. Gene expression levels were compared with WT mice at P4. Data
567 represent the mean ± SD. **P*<0.05 and ***P*<0.01 without a bar indicate the
568 comparison to WT mice at P4. n.s., not significant.

569

570 **FIG 7** Loss of the *Artn* distal enhancer reduces touch-evoked scratching behavior in
571 AhR-CA mice. (A) Dermatitis score of WT (n=5), Artn$^{\Delta XRE}$ (n=5), AhR-CA (n=7) and
572 AhR-CA::Artn$^{\Delta XRE}$ mice (n=5). **P*<0.05 and ‡ *P*<0.01 indicate the comparison of WT
573 mice to AhR-CA::Artn$^{\Delta XRE}$ mice. † *P*<0.01 indicates the comparison of WT mice to
574 AhR-CA mice. n.s., not significant (AhR-CA mice vs AhR-CA::Artn$^{\Delta XRE}$ mice). (B)
575 Alloknesis scores of WT (n=3), Artn$^{\Delta XRE}$ (n=3), AhR-CA (n=5) and AhR-CA::Artn$^{\Delta XRE}$
576 mice (n=4). Note that the alloknesis of AhR-CA::Artn$^{\Delta XRE}$ mice is improved
577 significantly compared to that of AhR-CA mice. **P*<0.05, and ***P*<0.01 without a bar
578 indicate the comparison to WT mice.

579

580

581 **FIG 8** Application of an Artn-neutralizing antibody (Artn-ab) reduces continuous
582 scratching behavior in AhR-CA mice. Mice on ICR background received a
583 subcutaneous injection of an Artn-ab or IgG2a antibody (control) once a week from the
584 first week to 11 weeks of age. (A) Dermatitis scores of WT (IgG2a or Artn-ab; n=5
585 each) and AhR-CA mice (IgG2a or Artn-ab; n=6 each) were evaluated. † $P<0.01$
586 (IgG2a-injected AhR-CA mice vs IgG2a-injected WT mice), ‡ $P<0.01$
587 (Artn-ab-injected AhR-CA mice vs IgG2a-injected WT mice), n.s., not significant
588 (IgG2a-injected AhR-CA vs Artn-ab-injected AhR-CA mice). Data represent the mean
589 ± SD. (B) Time of scratching behavior (vertical lines) in two WT and AhR-CA mice
590 treated with IgG2a or Artn-ab. (C) Quantification of continuous scratching behavior
591 (scratching without an interval of >5 s between bouts) in the WT (IgG2a or Artn-ab;
592 n=5 each) and AhR-CA mice (IgG2a or Artn-ab; n=6 each). Note that continuous
593 scratching in Artn-ab treated AhR-CA mice is improved compared to that in
594 IgG2a-treated AhR-CA mice. *$P<0.05$, and **$P<0.01$ without a bar indicate the
595 comparison to IgG2a-treated WT mice.

596

597 **FIG 9** Schema of the AhR-mediated development of alloknesis in AD. AhR is
598 activated by PAHs in environmental pollutants. Activated AhR directly binds to the
599 XRE in the *Artn* distal enhancer and induces the expression of the *Artn* gene in
600 keratinocytes. Artn enhances the growth of peripheral nerves to induce
601 hyperinnervation of the epidermis, resulting in hypersensitivity to itch (alloknesis).

602

603 **REFERENCES**

604 1. Hahn ME. 1998. The aryl hydrocarbon receptor: a comparative perspective.
605 Comp Biochem Physiol C Pharmacol Toxicol Endocrinol 121:23–53.
606 2. Denison MS, Nagy SR. 2003. Activation of the aryl hydrocarbon receptor by
607 structurally diverse exogenous and endogenous chemicals. Annu Rev Pharmacol
608 Toxicol 43:309–334.
609 3. Kim KH, Jahan SA, Kabir E, Brown RJC. 2013. A review of airborne polycyclic
610 aromatic hydrocarbons (PAHs) and their human health effects. Environ Int
611 60:71–80.
612 4. Denison MS, Fisher JM, Whitlock JP. 1988. The DNA recognition site for the
613 dioxin-Ah receptor complex. Nucleotide sequence and functional analysis. J Biol
614 Chem 263:17221–17224.
615 5. Fujii-Kuriyama Y, Mimura J. 2005. Molecular mechanisms of AhR functions in
616 the regulation of cytochrome P450 genes. Biochem Biophys Res Commun
617 338:311–317.
618 6. Mimura J, Fujii-Kuriyama Y. 2003. Functional role of AhR in the expression of
619 toxic effects by TCDD. Biochim Biophys Acta 1619:263–268.
620 7. Yi O, Kwon HJ, Kim H, Ha M, Hong SJ, Hong YC, Leem JH, Sakong J, Lee CG,
621 Kim SY, Kang D. 2012. Effect of environmental tobacco smoke on atopic
622 dermatitis among children in Korea. Environ Res 113:40–45.
623 8. Pénard-Morand C, Raherison C, Charpin D, Kopferschmitt C, Lavaud F, Caillaud
624 D, Annesi-Maesano I. 2010. Long-term exposure to close-proximity air pollution
625 and asthma and allergies in urban children. Eur Respir J 36:33–40.
626 9. Morgenstern V, Zutavern A, Cyrys J, Brockow I, Koletzko S, Kramer U,
627 Behrendt H, Herbarth O, Von Berg A, Bauer CP, Wichmann HE, Heinrich J.
628 2008. Atopic diseases, allergic sensitization, and exposure to traffic-related air
629 pollution in children. Am J Respir Crit Care Med 177:1331–1337.
630 10. Kim YM, Kim J, Han Y, Jeon BH, Cheong HK, Ahn K. 2017. Short-term effects
631 of weather and air pollution on atopic dermatitis symptoms in children: A panel
632 study in Korea. PLoS One 12:1–13.
633 11. Eberlein-König B, Przybilla B, Kühnl P, Pechak J, Gebefügi I, Kleinschmidt J,
634 Ring J. 1998. Influence of airborne nitrogen dioxide or formaldehyde on
635 parameters of skin function and cellular activation in patients with atopic eczema
636 and control subjects. J Allergy Clin Immunol 101:141–143.
637 12. Tauchi M, Hida A, Negishi T, Katsuoka F, Noda S, Mimura J, Hosoya T, Yanaka
638 A, Aburatani H, Fujii-kuriyama Y, Motohashi H, Yamamoto M. 2005.

639 Constitutive expression of aryl hydrocarbon receptor in keratinocytes causes
640 inflammatory skin lesions. Mol Cell Biol 25:9360–9368.
641 13. Hidaka T, Ogawa E, Kobayashi EH, Suzuki T, Funayama R, Nagashima T,
642 Fujimura T, Aiba S, Nakayama K, Okuyama R, Yamamoto M. 2017. The aryl
643 hydrocarbon receptor AhR links atopic dermatitis and air pollution via induction
644 of the neurotrophic factor artemin. Nat Immunol 18:64–73.
645 14. Akiyama T, Carstens MI, Ikoma A, Cevikbas F, Steinhoff M, Carstens E. 2012.
646 Mouse model of touch-evoked itch (alloknesis). J Invest Dermatol 132:1886–
647 1891.
648 15. Mack MR, Kim BS. 2018. The itch-scratch cycle: a neuroimmune perspective.
649 Trends Immunol 39:980–991.
650 16. Baloh RH, Tansey MG, Lampe PA, Fahrner TJ, Enomoto H, Simburger KS,
651 Leitner ML, Araki T, Johnson EM, Milbrandt J. 1998. Artemin, a novel member
652 of the GDNF ligand family, supports peripheral and central neurons and signals
653 through the GFRα3-RET receptor complex. Neuron 21:1291–1302.
654 17. Molliver DC, McIlwrath SL, Cornuet PK, Davis BM, Albers KM, Lawson JJ,
655 Elitt CM, Malin SA, Koerber HR. 2006. Artemin overexpression in skin
656 enhances expression of TRPV1 and TRPA1 in cutaneous sensory neurons and
657 leads to behavioral sensitivity to heat and cold. J Neurosci 26:8578–8587.
658 18. Riddick DS, Huang Y, Harper PA, Okey AB. 1994.
659 2,3,7,8-Tetrachlorodibenzo-p-dioxin versus 3-methylcholanthrene: Comparative
660 studies of Ah receptor binding, transformation, and induction of CYP1A1. J Biol
661 Chem 269:12118–12128.
662 19. Thornton P, Hatcher JP, Robinson I, Sargent B, Franzén B, Martino G, Kitching
663 L, Glover CP, Anderson D, Forsmo-Bruce H, Low CP, Cusdin F, Dosanjh B,
664 Williams W, Steffen AC, Thompson S, Eklund M, Lloyd C, Chessell I, Hughes J.
665 2013. Artemin-GFRα3 interactions partially contribute to acute inflammatory
666 hypersensitivity. Neurosci Lett 545:23–28.
667 20. Fujisawa-Sehara A, Sogawa K, Yamane M, Fujii-Kuriyama Y. 1987.
668 Characterization of xenobiotic responsive elements upstream from the
669 drug-metabolizing cytochrome p-450c gene: A similarity to glucocorticoid
670 regulatory elements. Nucleic Acids Res 15:4179–4191.
671 21. Tsuchiya Y, Nakajima M, Yokoi T. 2003. Human enhancer region gene to which
672 AhR/ARNT and bind in the human CYP1B gene. J Biochem 592:583–592.
673 22. Kress S, Reichert J, Schwarz M. 1998. Functional analysis of the human
674 cytochrome P4501A1 (CYP1A1) gene enhancer. Eur J Biochem 258:803–812.

675 23. Lo R, Matthews J. 2012. High-resolution genome-wide mapping of AHR and
676 ARNT binding sites by ChIP-Seq. Toxicol Sci 130:349–361.
677 24. Haarmann-stemmann T, Bothe H, Kohli A, Sydlik U, Abel J, Fritsche E. 2007.
678 Analysis of the transcriptional regulation and molecular function of the aryl
679 hydrocarbon receptor repressor in human cell lines. Drug Metab Dispos 35:2262–
680 2269.
681 25. Pandey V, Zhu T, Liu DX, Miller LD, Liu ET, Perry JK, Kang J, Qian PX, Lobie
682 PE. 2010. Artemin is estrogen regulated and mediates antiestrogen resistance in
683 mammary carcinoma. Oncogene 29:3228–3240.
684 26. Matthews J, Gustafsson JA. 2006. Estrogen receptor and aryl hydrocarbon
685 receptor signaling pathways. Nucl Recept Signal 4:e016.
686 27. Ohtake F, Takeyama K, Matsumoto T. 2003. Modulation of oestrogen receptor
687 signalling by association with the activated dioxin receptor. Nature 1:545–550.
688 28. Abdelrahim M, Ariazi E, Kim K, Khan S, Barhoumi R, Burghardt R, Liu S, Hill
689 D, Finnell R, Wlodarczyk B, Jordan VC, Safe S. 2006. 3-Methylcholanthrene and
690 other aryl hydrocarbon receptor agonists directly activate estrogen receptor α.
691 Cancer Res 66:2459–2467.
692 29. Verdier-Sevrain S, Yaar M, Cantatore J, Traish A, Gilchrest BA. 2004. Estradiol
693 induces proliferation of keratinocytes via a receptor mediated mechanism.
694 FASEB J 18:1252–1254.
695 30. Verdier-Sévrain S, Bonté F, Gilchrest B. 2006. Biology of estrogens in skin:
696 Implications for skin aging. Exp Dermatol 15:83–94.
697 31. Darsow U, Wollenberg A, Simon D, Taïeb A, Werfel T, Oranje A, Gelmetti C,
698 Svensson A, Deleuran M, Calza A-M, Giusti F, Lübbe J, Seidenari S, Ring J.
699 2009. ETFAD/EADV eczema task force 2009 position paper on diagnosis and
700 treatment of atopic dermatitis. J Eur Acad Dermatology Venereol 24:317–328.
701 32. Elmariah SB, Lerner EA. 2011. Topical therapies for pruritus. Semin Cutan Med
702 Surg 30:118–126.
703 33. Walisser JA, Glover E, Pande K, Liss AL, Bradfield CA. 2005. Aryl hydrocarbon
704 receptor-dependent liver development and hepatotoxicity are mediated by
705 different cell types. Proc Natl Acad Sci U S A 102:17858–17863.
706 34. Tarutani M, Itami S, Okabe M, Ikawa M, Tezuka T. 1997. Tissue-specific
707 knockout of the mouse Pig-a gene reveals important roles for GPI-anchored
708 proteins in skin development. Proc Natl Acad Sci U S A 94:7400–74005.
709 35. Yamamura K, Uruno T, Shiraishi A, Tanaka Y, Ushijima M, Nakahara T,
710 Watanabe M, Kido-Nakahara M, Tsuge I, Furue M, Fukui Y. 2017. The

711 transcription factor EPAS1 links DOCK8 deficiency to atopic skin inflammation
712 via IL-31 induction. Nat Commun 8:13946.
713 36. Kuraishi Y, Nagasawa T, Hayashi K, Satoh M. 1995. Scratching behavior
714 induced by pruritogenic but not algesiogenic agents in mice. Eur J Pharmacol
715 275:229–233.
716 37. Manzella C, Singhal M, Alrefai WA, Saksena S, Dudeja PK, Gill RK. 2018.
717 Serotonin is an endogenous regulator of intestinal CYP1A1 via AhR. Sci Rep
718 8:1–13.
719 38. Taguchi K, Maher JM, Suzuki T, Kawatani Y, Motohashi H, Yamamoto M. 2010.
720 Genetic analysis of cytoprotective functions supported by graded expression of
721 Keap1. Mol Cell Biol 30:3016–3026.
722

FIG 1

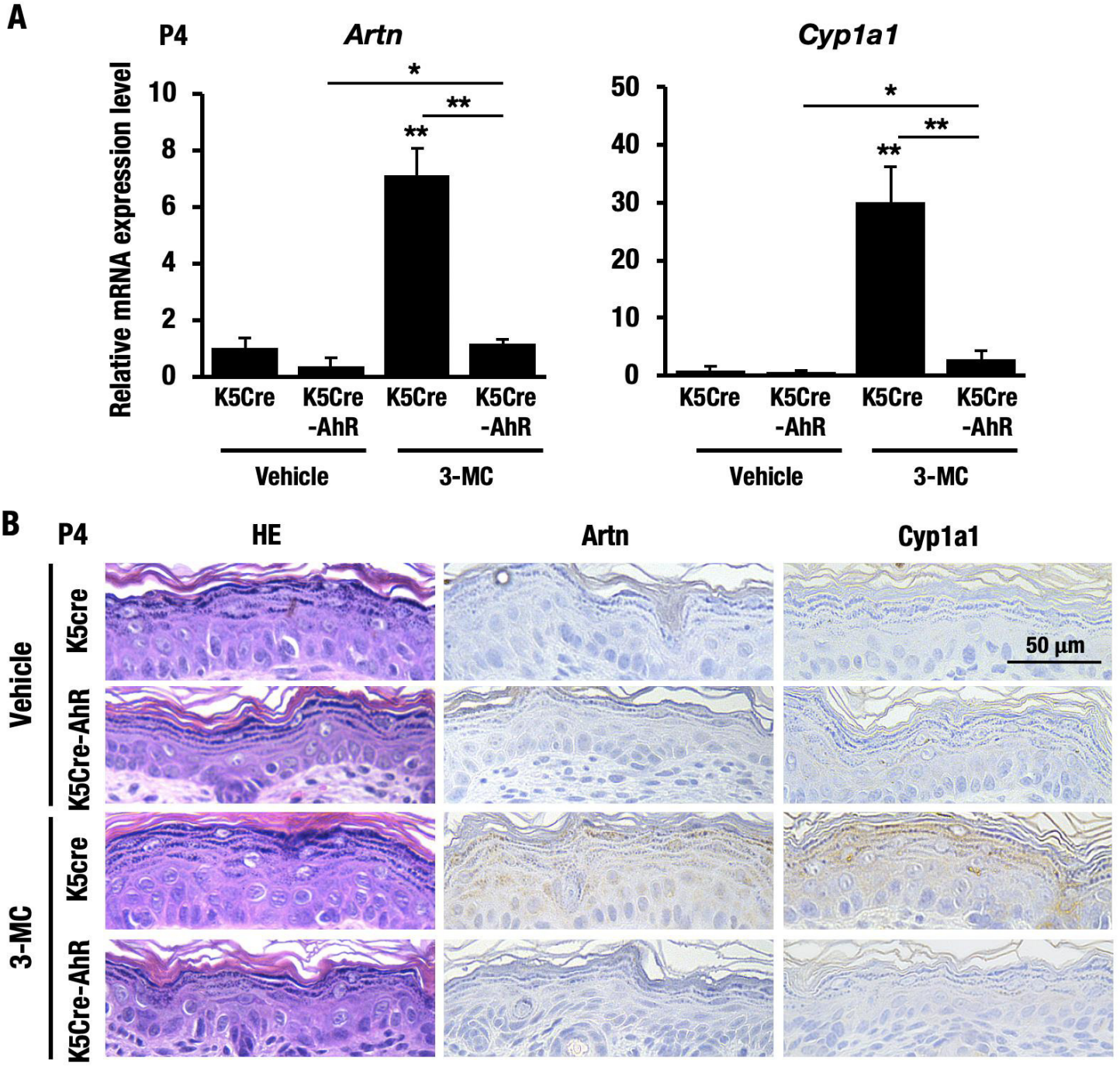
A
P4
Artn
Cyp1a1
Relative mRNA expression level
10
8
6
4
2
0
50
40
30
20
10
0
*
**
**
K5Cre
K5Cre -AhR
K5Cre
K5Cre -AhR
Vehicle
3-MC
B
P4
HE
Artn
Cyp1a1
Vehicle
3-MC
K5cre
K5Cre-AhR
K5cre
K5Cre-AhR
50 µm

FIG 2

A

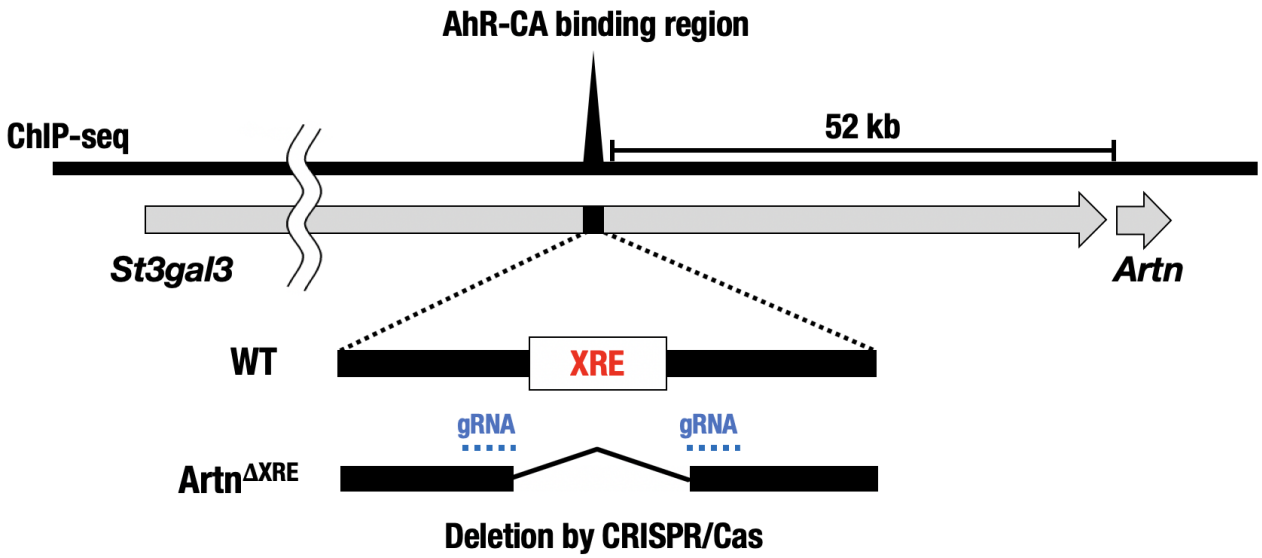

B

Chromosome 4, 117,982,819–117,982,973

```
                PAM        gRNA                XRE      PAM        gRNA
WT      | 5'- CTACCTCCCCGGTTGCTGTAGAGAGG---CACGC---TCCCTTCGTGCACAGGGAGTGCCAGGTC -3'
ArtnΔXRE
        | #1  5'- CTACCTCCC-------------------(Δ128 bp)--------------------CACAGGGAGTGCCAGGTC -3'
        | #2  5'- CTACCTCCC-------------------(Δ126 bp)-----------------TGCACAGGGAGTGCCAGGTC -3'
```

C

FIG 3

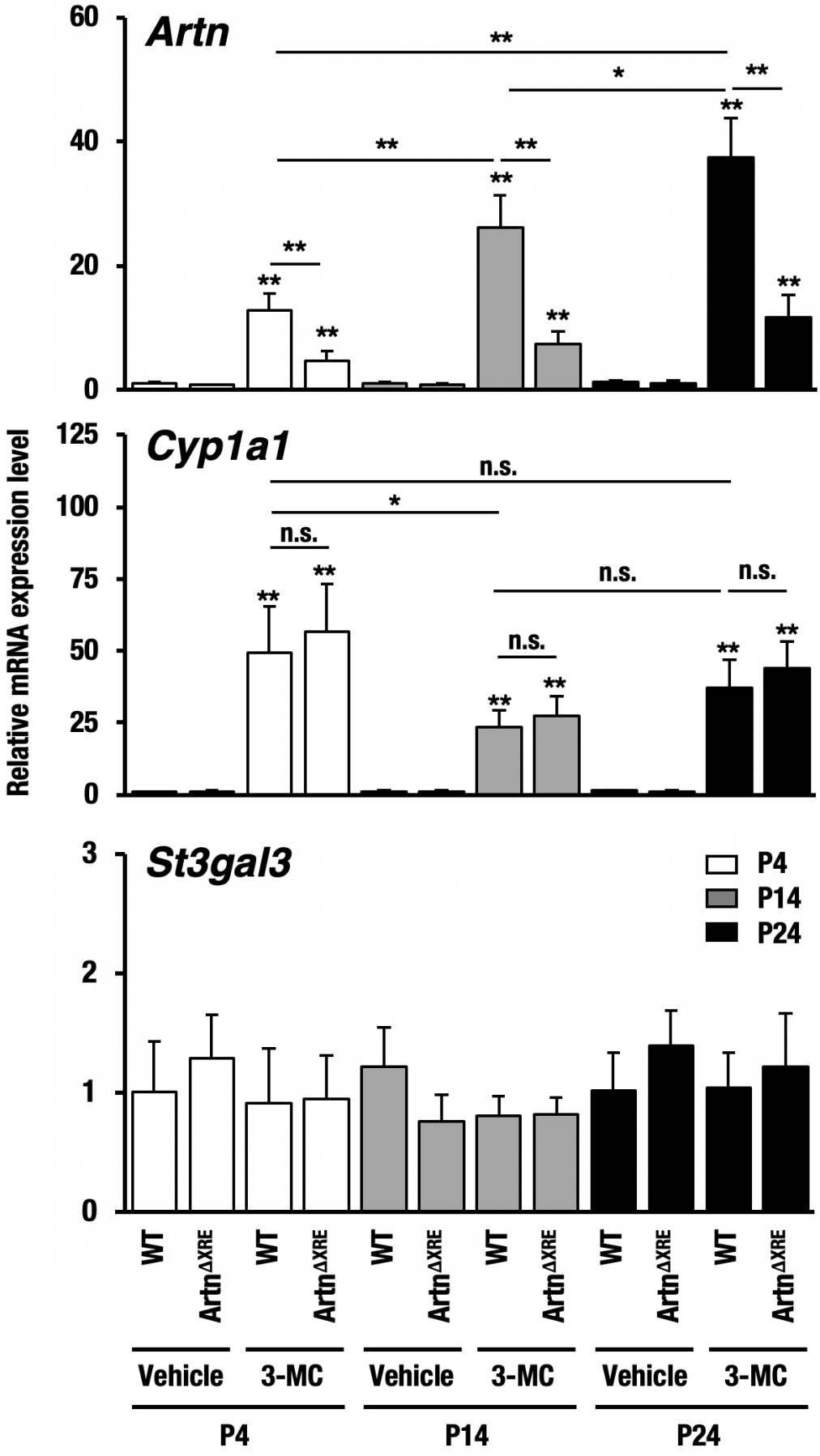
Artn
Cyp1a1
St3gal3
Relative mRNA expression level
P4
P14
P24
WT
ArtnΔXRE
Vehicle
3-MC
n.s.

FIG 4

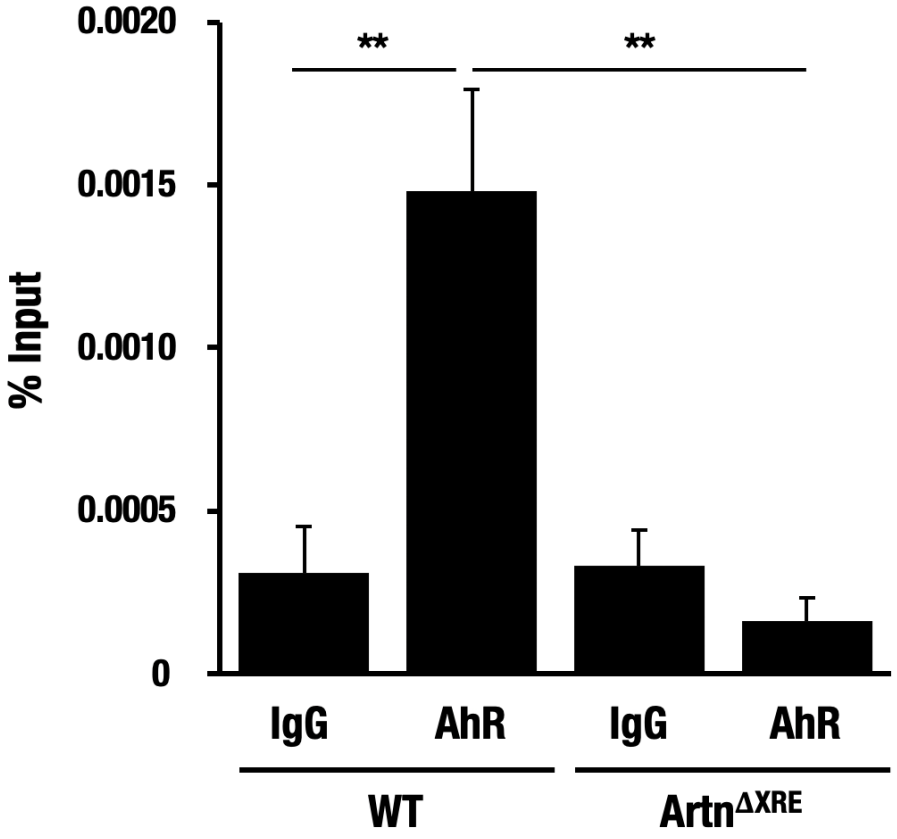
0.0020
0.0015
0.0010
0.0005
0
% Input
**
**
IgG
AhR
IgG
AhR
WT
Artn$^{\Delta XRE}$

FIG 5

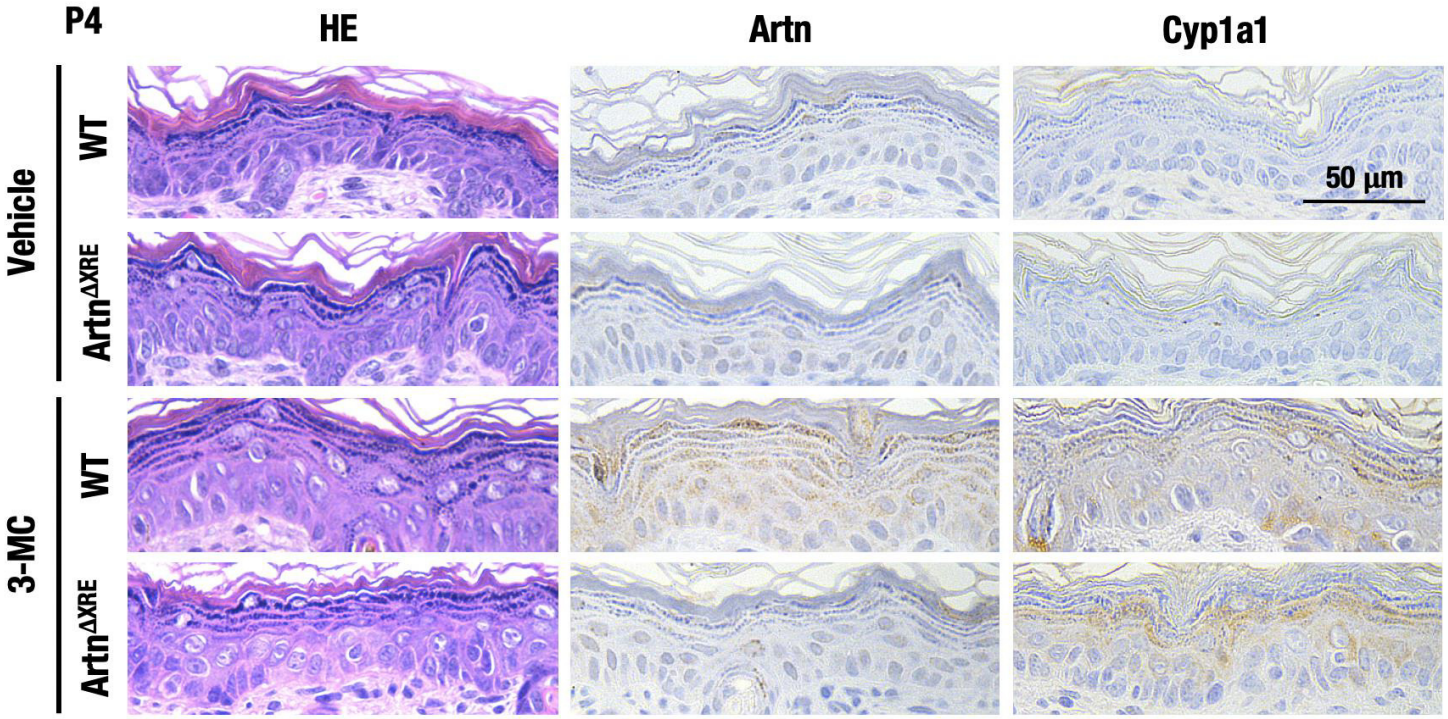
P4
HE
Artn
Cyp1a1
Vehicle
WT
Artn$^{\Delta XRE}$
3-MC
WT
Artn$^{\Delta XRE}$
50 µm

FIG 6

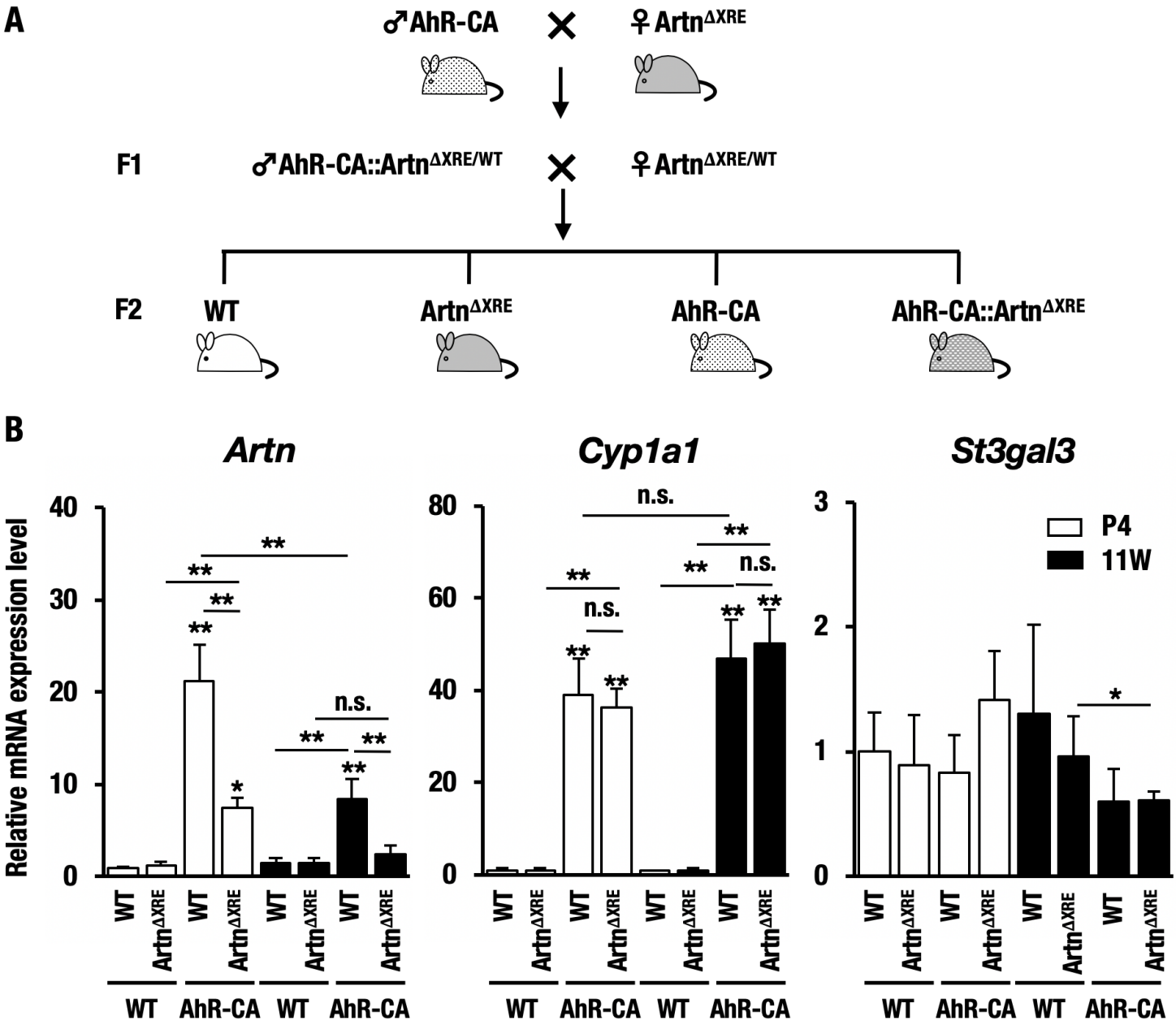
A
♂AhR-CA
×
♀Artn^ΔXRE
F1
♂AhR-CA::Artn^ΔXRE/WT
×
♀Artn^ΔXRE/WT
F2
WT
Artn^ΔXRE
AhR-CA
AhR-CA::Artn^ΔXRE
B
Artn
Cyp1a1
St3gal3
Relative mRNA expression level
P4
11W
n.s.
WT
Artn^ΔXRE
AhR-CA

FIG 7

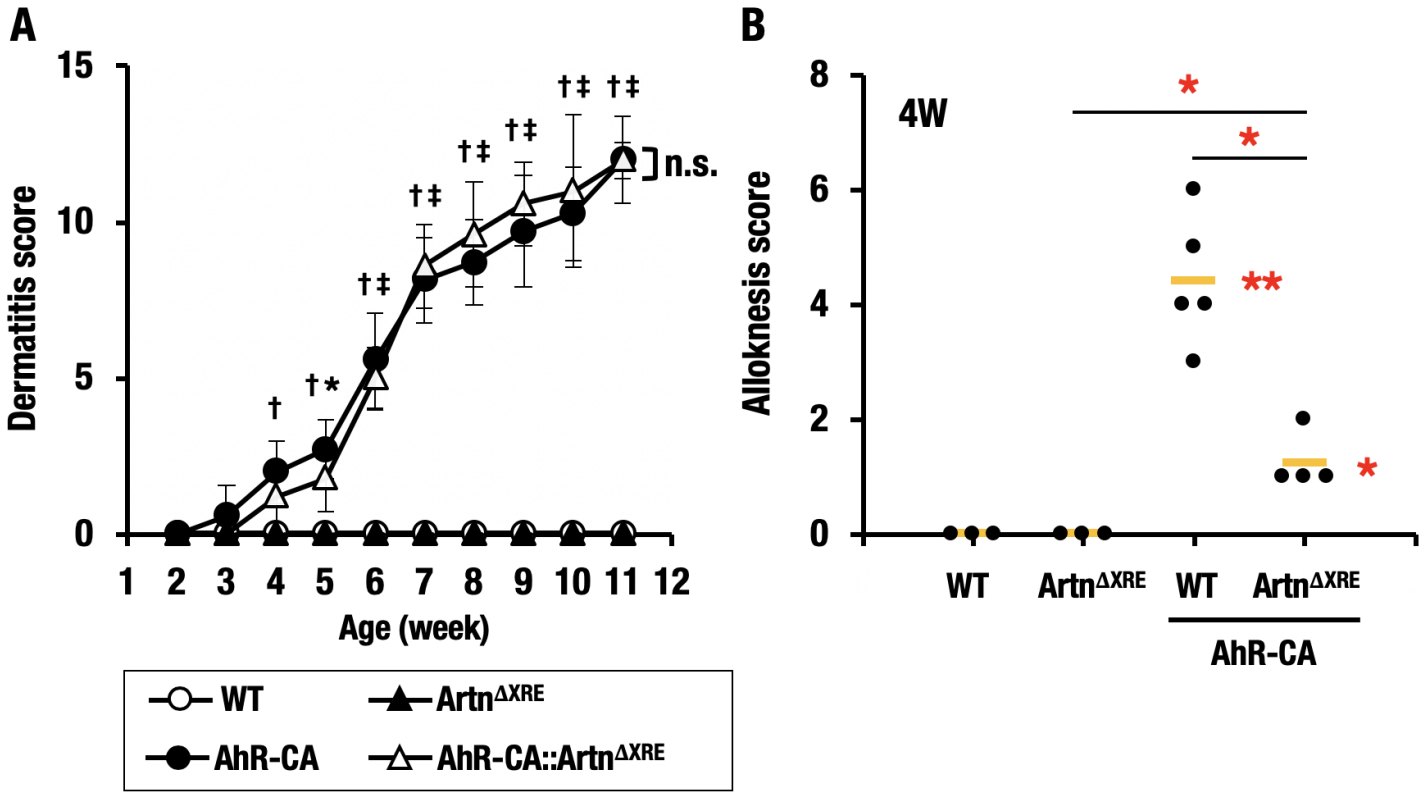
A
Dermatitis score
15
10
5
0
1 2 3 4 5 6 7 8 9 10 11 12
Age (week)
†
†*
†‡
n.s.
WT
Artn^ΔXRE
AhR-CA
AhR-CA::Artn^ΔXRE
B
Alloknesis score
8
6
4
2
0
4W
*
**
WT
Artn^ΔXRE
WT
Artn^ΔXRE
AhR-CA

FIG 8

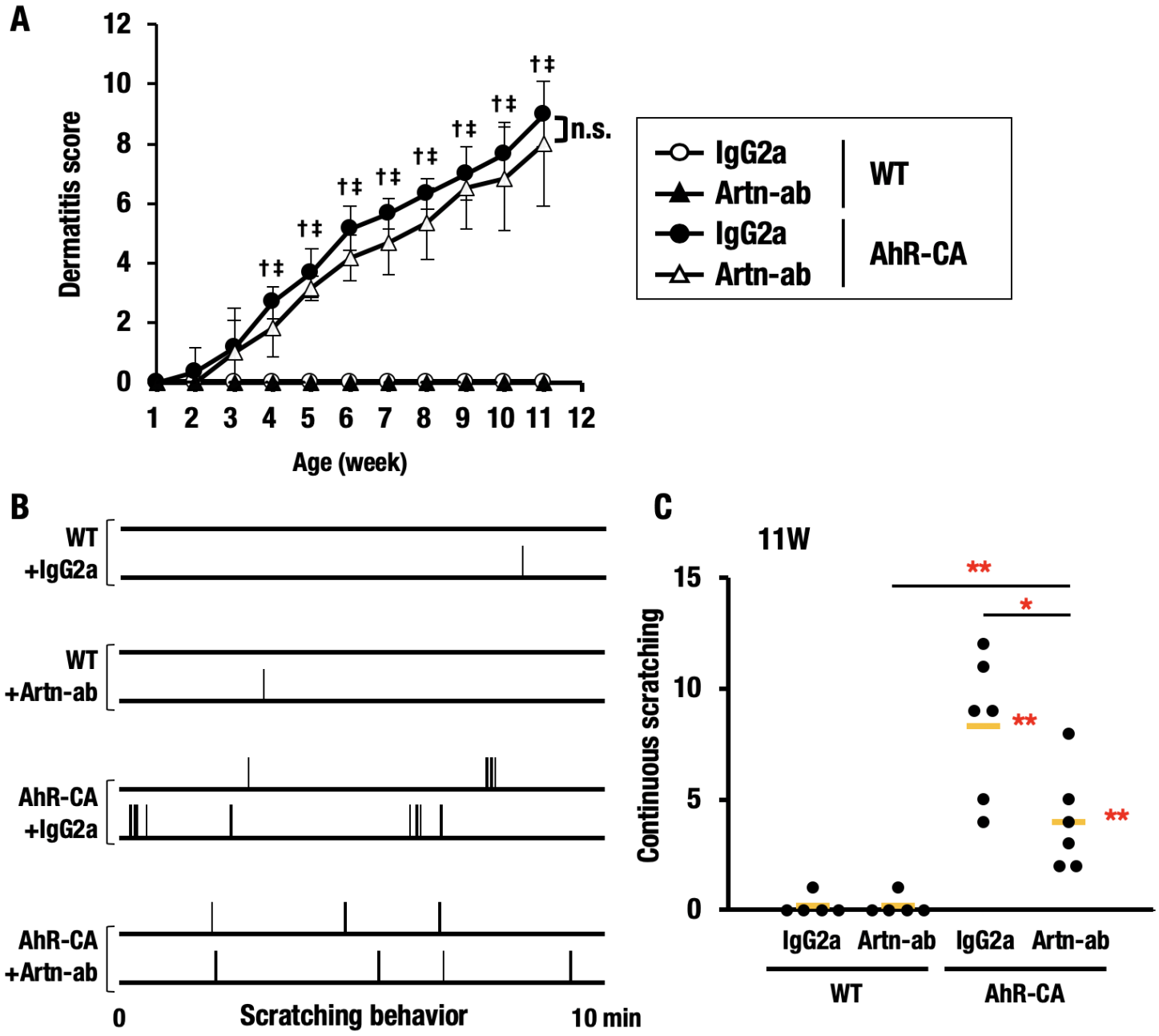
A
Dermatitis score
Age (week)
n.s.
IgG2a
Artn-ab
WT
IgG2a
Artn-ab
AhR-CA
B
WT +IgG2a
WT +Artn-ab
AhR-CA +IgG2a
AhR-CA +Artn-ab
0
Scratching behavior
10 min
C
11W
Continuous scratching
IgG2a
Artn-ab
IgG2a
Artn-ab
WT
AhR-CA

FIG 9

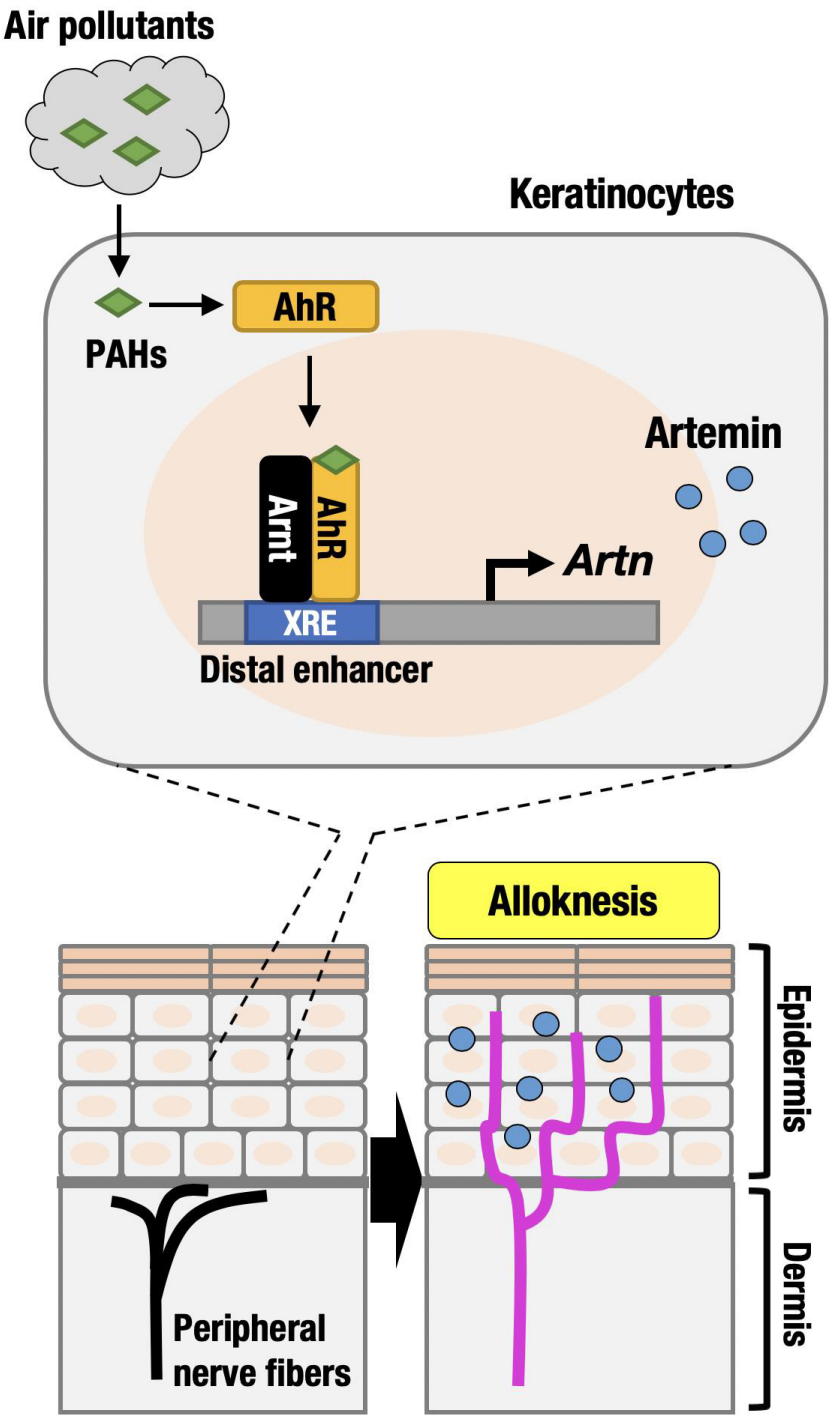
Air pollutants
Keratinocytes
AhR
PAHs
Arnt
AhR
Artemin
Artn
XRE
Distal enhancer
Alloknesis
Epidermis
Dermis
Peripheral
nerve fibers